RSC Advances

This is an *Accepted Manuscript*, which has been through the Royal Society of Chemistry peer review process and has been accepted for publication.

Accepted Manuscripts are published online shortly after acceptance, before technical editing, formatting and proof reading. Using this free service, authors can make their results available to the community, in citable form, before we publish the edited article. This *Accepted Manuscript* will be replaced by the edited, formatted and paginated article as soon as this is available.

You can find more information about *Accepted Manuscripts* in the Information for Authors.

Please note that technical editing may introduce minor changes to the text and/or graphics, which may alter content. The journal's standard Terms & Conditions and the Ethical guidelines still apply. In no event shall the Royal Society of Chemistry be held responsible for any errors or omissions in this *Accepted Manuscript* or any consequences arising from the use of any information it contains.

ROYAL SOCIETY OF CHEMISTRY

www.rsc.org/advances

ARTICLE TYPE www. rsc.org/xxxxxx | XXXXXXXX

The investigation of transition metal doped $CuGaS_2$ for promising intermediate band materials

Miaomiao Han,[a,b] **Xiaoli Zhang,**[b] **and Z. Zeng,**[*a,b]

Received Xth XXXXXXXXXX 20XX, Accepted Xth XXXXXXXXX 20XX
First published on the web Xth XXXXXXXXXX 200X
DOI: 10.1039/b000000x

Using the density functional theory by considering the non-local interaction, here we have systematically investigated the electronic structure and optical properties of transition metal *M* doped $CuGaS_2$ (*M* = Fe, Co, Ni) systems. Isolated intermediate bands (IBs), with the potential of achieving the efficiency of photovoltaic materials, are introduced in the main bandgap of host $CuGaS_2$ by doping Fe or Ni with the favorable position and width. Therefore, extra absorption peaks appear in the optical spectrum of Fe or Ni doped $CuGaS_2$ compound, accompanied with greatly enhanced light absorption intensity and largely broadened light absorption energy range. Whereas, for Co doped $CuGaS_2$, the material turns into a half-metal. Consequently, Fe or Ni doped $CuGaS_2$ could be potential materials for future applications in photovoltaic area.

1 Introduction

The concept of intermediate band solar cell (IBSC) was first put forward in an attempt to increase the efficiency of solar cells by making full use of solar energy in 1997. Traditionally, the absorption layer of solar cell is a single band gap semiconductor, where electrons are directly promoted from the valence band (VB) to the conduction band (CB) by absorbing photons. While, a three-photon absorption process happens when inserting a partially filled intermediate band (IB) into the forbidden bandgap. As shown in Fig. 1, electrons can be excited not only from the VB to the CB but also from IB to CB and from VB to IB respectively. As IB is isolated, the IBSC will have a higher photocurrent benefited from sub-bandgap absorption without photo-voltage degradation, which promises high conversion efficiencies. The upper limit efficiency of IBSC was predicted to be about 63.1% from the detailed balance limit theory calculation,[1] which largely exceeds the efficiency of Shockley-Queisser single-junction solar cell (40.7%).[2] By further increasing the number of IBs, the efficiency will be extended to nearly 80%.[3] Theoretical and experimental reports have verified that IB materials could effectively increase the optical absorption.[4–6]

Since the IB concept was proposed, large efforts have been made in implementation of IB solar cells. In practice, the IB can be created through quantum dots or the insertion of appropriate impurities into bulk host semiconductor, in which the bulk IB material is easier to fabricate than quantum dots and has a stronger absorption because of the higher density of IB states.[7] The candidate bulk IB host materials contain III-V,[8,9] II-VI,[10] spinel compounds[11] and chalcopyrite materials. In particular, it has been reported that the optimum bandgap of Cu-based chalcopyrite solar cells for photovoltaic energy conversion is 2.41 eV with the IB located at 0.92 eV from the CB or VB.[12] $CuGaS_2$[13] has a relatively wide bandgap of 2.43 eV, thus being an ideal IB host material[12] though not suitable to act as a light absorption layer in single-junction solar cell. Up to now, many first-principles calculations based on density functional theory (DFT)[14,15] have been made to design and understand the bulk $CuGaS_2$ IB materials. Elements of 3*d* transition metal and group IVA have been identified as interesting candidates to act as substitutes in the cation sites of the $CuGaS_2$ chalcopyrite hosts.[15–17] It is worth noting that Ti,[18] Sn[19] and Fe-doped $CuGaS_2$ IB semiconductors have been successfully synthesized and that sub-gap transitions are detected in photovoltaic devices based on Fe-doped $CuGaS_2$.[20] There are many literatures about Ti, V, Cr, Mn

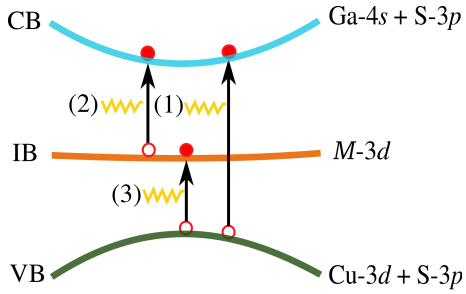

Fig. 1 Schematically show of band diagram of an IBSC. (1) (2) and (3) represent photon absorptions.

[a] *Key Laboratory of Materials Physics, Institute of Solid State Physics, Chinese Academy of Sciences, Hefei 230031, China*
[b] *University of Science and Technology of China, Hefei 230026, China*
[*] *Email: zzeng@theory.issp.ac.cn; Tel: +86-551-65591407; Fax: +86-551-65591434*

RSC Advances Accepted Manuscript

and group IVA doped $CuGaS_2$ too.[15–19,21–23] Nevertheless, seldom systematic theoretical study of Fe, Co and Ni doped $CuGaS_2$ has ever been made. The key factor in IBSC is that IB must be isolated. Whereas for the issue of isolated IB, no consistent conclusion has been drawn from theoretical calculations by using GGA and GGA + U. Taking Ti-doped $CuGaS_2$ for example, the GGA calculation results[14] show that the partially filled IB little overlaps with CB, while the GGA + U[14] shows that the IB is filled. The contradiction is inherent of DFT, because is well known that DFT underestimates the bandgaps of materials and that the position and width of IB is not reliable, which is severely harmful to predicting the optical properties of IB materials. Therefore, an advanced theoretical method should be used to provide a more accurate description of the electronic and optical properties of IB semiconductors. Attractively, the range-separated hybrid functional of Heyd-Scuseria-Ernzerhof (HSE06) makes the exact exchange mixing with exchange from a semilocal Perdew-Burke-Ernzerhof generalized gradient approximation (PBE-GGA) functional, thereby overcoming the problems in GGA and LDA that *d* and *f* electrons are handled improperly due to insufficient electron correlations and relativistic effects. The investigations have indicated that hybrid functionals can describe the bandgap of such chalcopyrite systems very well.[24,25]

In this work, we employ screened-exchange hybrid density functional HSE06 in the calculation of electronic structure and optical properties of *M* (*M* = Fe, Co, Ni) doped $CuGaS_2$. The band gap of $CuGaS_2$ we calculate is 2.01 eV, in good agreement with the experimental value 2.43 eV.[26] Our results show that the *M* doped $CuGaS_2$ exhibit a good IB concept with IB states appearing in the bandgap. Consequently, two additional absorption peaks appear in the absorption spectrum around 1.0 eV and 1.7 eV when $CuGaS_2$ is doped with Fe, arising from the sub-gap absorptions, which is in consistent with the experimental results.[20,27] Additionally, the Ni dopant induces isolated IB states slightly above the valence band. For both Fe and Ni doping, the optical absorptions are greatly enhanced compared with the host $CuGaS_2$. Conversely, the IBs induced by Co dopant overlap with the conduction band, with the doped material developing into a half-metal. Our results explicitly indicate that $CuGa_{1-x}M_xS_2$ system, with *M* = Fe or Ni, is a potential candidate for the IB photovoltaic material.

2 Model and method

2.1 Theoretical model

The ternary semiconductor $CuGaS_2$ is a chalcopyrite structure with the space group of $I\bar{4}2d$. Each atom in this structure is fourfold coordinated. Namely, each sulfur ion is coordinated with two gallium and two copper ions, and each cation is coordinated with four sulfur ions. The supercell approach is used to construct the compound by replacing one Ga atom with *M* (*M* = Fe, Co, Ni) dopant in a 16-atom cell (see Fig.2), which corresponds to the 25% dopant concentration. In this case, the concentration of dopant *M* equals to 3.3×10^{21} cm^{-3}, which is in the optimal range of 10^{21} cm^{-3} that the Shockley-Read-Hall (SRH) recombination might be suppressed.[28]

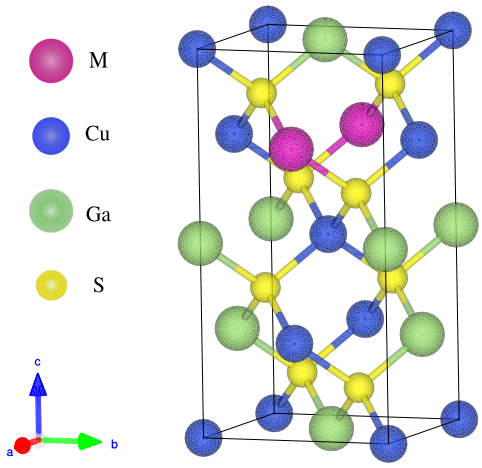

Fig. 2 The crystal structure of *M* (Fe, Co, Ni) doped $CuGaS_2$.

2.2 Computational method

The whole investigation is performed within the framework of density functional theory (DFT) implemented in the Vienna ab initio simulation package (VASP).[29] Previous studies indicate that hybrid functionals can describe such chalcopyrite systems very well.[24,25] However, relaxation and electronic structure calculation using Heyd-Scuseria-Ernzerhof (HSE06) are very time consuming. We test the geometry optimization for Fe-doped case within HSE06 and Perde-Burke-Ernzerhof (PBE).[30] The results show that PBE relaxed structure can capture the main properties of electronic structure. Therefore, for the exchange correlation functional, the PBE version of the generalized gradient approximation (GGA) is used for full structure relaxation, while the hybrid nonlocal exchange-correlation functional of HSE06 is used to calculate the electronic structure and optical properties. The projector augmented wave (PAW)[31] method has been used to describe the inert core electrons. In the HSE06[32,33] functional, 25% of screened Hartree-Fock (HF) exchange is mixed to PBE exchange functional and the screening parameter is set to 0.2 $Å^{-1}$. The relaxation is performed until the total energy changed within 0.0001 eV/atom and the Hellmann-Feynman force on each atomic site is less than 0.01 eV/Å. The cutoff energy for the plane-wave basis is set to 400 eV. We apply

RSC Advances Accepted Manuscript

This journal is © The Royal Society of Chemistry [year]

6×6×3 Γ-centered Monkhorst-Pack[34] k-point mesh in both PBE and HSE calculations. Spin polarization is concerned due to the existence of magnetic *M* (Fe, Co, Ni) atom.

To get a better prediction in both the intensities and the peak positions in the optical absorption spectrum, a complex dielectric function is performed using the HSE06 with the consideration of interband and direct transitions, but not the local-field effects. The optical calculations count the contribution from 300 electronic bands.

3 Results and discussions

3.1 Structural and electronic properties

The optimized structure of host $CuGaS_2$ compound presents an average bond length of Ga-S of 2.32 Å, which is in consistent with previous theoretical and experimental values.[35] The doping of *M* into the host $CuGaS_2$ leads to the decreasing of *M*-S bond lengths, as shown in table 1. The bond lengths decrease to 2.29 Å , 2.24 Å and 2.23 Å for Fe-S, Co-S and Ni-S in *M*-doped $CuGaS_2$, respectively. The magnitude of the bond length is determined by the size mismatch between Fe/Co/Ni and Ga ions. The bond lengths decreasing of Ga-S and Cu-S in *M*-doped $CuGaS_2$ are much smaller compared with that of *M*-S about 0.01 Å. The characteristics of structure change in *M*-doped $CuGaS_2$ indicate that the *M* dopant mainly alter the local structure around the *M* ions.

Table 1 Lattice parameter a, bond lengths d (in Å) and band gaps E_g (in eV) of host $CuGaS_2$ and *M* doped $CuGaS_2$ after relaxation.

	a	d_{Ga-S}	d_{Cu-S}	d_{M-S}	E_g
$CuGaS_2$	5.36	2.32	2.31	–	2.01
$Cu_4Ga_3FeS_8$	5.34	2.31	2.30	2.29	2.14
$Cu_4Ga_3CoS_8$	5.32	2.31	2.30	2.24	2.19
$Cu_4Ga_3NiS_8$	5.31	2.31	2.30	2.23	2.27

The structure changes for *M*-doped $CuGaS_2$ are accompanied with the electronic structure changes, as shown in Fig. 3. The band structure of host $CuGaS_2$ shows a direct bandgap at the Γ point of 2.01 eV, which is larger than the previous DFT computational results within LDA/GGA scheme (0.68 eV ∼ 1.25 eV[4,35–37]) and close to the experimental value of about 2.43 eV. The spin polarized band structures are plotted for *M*-doped $CuGaS_2$ in Fig. 3 owing to the magnetic nature of *M* ions. The most obvious change of the band structures with the doping of *M* ions is the appearance of additional IBs in the band gap. The IBs are contributed by the down spin states with 5, 3, and 3 bands for Fe, Co and Ni doped $CuGaS_2$ respectively. Regarding the up spin, it can be seen from Fig. 3 that Fe and Ni dopant do not change the host band structure much but Co dopant greatly change the band structure of the host material with an up shift of the valence band. This shifting makes Co doped $CuGaS_2$ be a half-metal. The IB induced by Fe and Ni divides the main band gap into two subbands and therefore may benefit for solar cell performance. The main gaps for Fe and Ni doped $CuGaS_2$ are 2.14 and 2.17 eV, with a little brodening as presented in table 1, which can be explained by the energy level repulsion between IBs and conduction band maximum (CBM). In order to have a better understanding of the origin of IB, we show the density of states (DOS) and projected density of states (PDOS) in Fig. 4.

The IB is mainly contributed from the *M*-3*d* states, as seen from the PDOS of *M*-doped $CuGaS_2$ in Fig. 4(b). Whereas, the IB states also contain small amount of the 3*p* states of neighboring S atoms and 3*d* states of Cu atoms because of the weak hybridization among *M*, Cu and S ions. The IBs for Fe-doped $CuGaS_2$ locate at the energy region from 1.05 eV to 1.76 eV, with a width of 0.71 eV. We also perform one case of Fe for the concentration of 12.5% and 6.25% so as to get the effect of dopant concentration. The results suggest that the use of larger supercells only slightly changes the positions of IBs but the IBs are still isolated, which do not change our main conclusions. Therefore the use of 16-atom supercell is reasonable. The IBs induced by Co dopant up shift and overlap with the CBM. This is a little different from the reported LSDA results that an isolated IB appears in the bandgap,[37] which may be caused by either the real nature of the material or the computational method deviation. The IBs induced by Ni are slightly lower than that by Fe ranging from 0.23 eV to 1.16 eV with a width of 0.93 eV. The *M* induced IBs is stronger for Fe than that for Co and Ni. Moreover, the up-spin states for Fe, Co and Ni are almost fully occupied, while the down-spin states are empty for Fe, and partially occupied for Co and Ni. The differences in PDOS for *M*-doped $CuGaS_2$ can be understood from the atomic environment and the 3*d* electron configurations of *M* ions, as will be discussed below.

In chalcopyrite $CuGaS_2$, the four nearest neighbor S atoms around the Ga atom form a tetrahedral crystal field. The *M* ions substitute the Ga atom in $CuGaS_2$ and therefore locate in a tetrahedral crystal field environment. Based on the crystal field theory, the five-fold degenerated 3*d* orbital of *M* will split into two main manifolds: a lower two-fold degenerate e_g states (d_{z^2}, $d_{x^2-y^2}$) and an upper three-fold degenerate t_{2g} states (d_{xy}, d_{yz}, d_{xz}). In addition, it is usual to take $CuGaS_2$ as an ionic compound for convenience where the Ga atom has the formal charge Ga^{3+}. The substituting of Ga with *M* leads to M^{3+} oxidation state, with the number of *d* electrons to be $Fe^{3+}(d^5)$, $Co^{3+}(d^6)$, $Ni^{3+}(d^7)$, respectively. The orbital split-

RSC Advances Accepted Manuscript

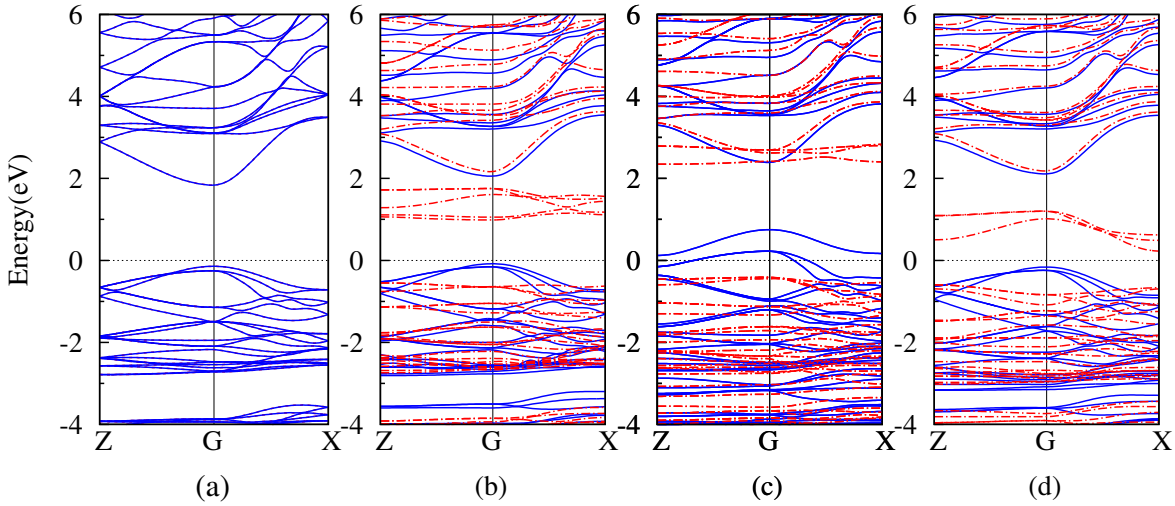

Fig. 3 Spin polarized band structures of (a) host $CuGaS_2$ (b) Fe (c) Co (d) Ni doped $CuGaS_2$ respectively. The solid (blue)/dashed(red) line denotes spin up/down. The horizontal dash line denotes the Fermi level.

ting in tetrahedral crystal field combined with the PDOS of *M*-3*d* leads to the Fe^{3+} $3d^5$ $e_g^{2\uparrow}$ $t_{2g}^{3\uparrow}$, Co^{3+} $3d^6$ $e_g^{2\uparrow}$ $t_{2g}^{3\uparrow}$ $e_g^{\downarrow}$, Ni^{3+} $3d^7$ $e_g^{2\uparrow}$ $t_{2g}^{3\uparrow}$ $e_g^{2\downarrow}$ orbital occupations as schematically shown in Fig. 5. These orbital occupations indicate that the crystal field splitting of e_g and t_{2g} are small and therefore the orbital occupation of *d* electrons obey the Hund's rule. The corresponding magnetic moments of these configurations should be 5 μ_B, 4 μ_B, 3μ_B for Fe, Co, Ni atoms, respectively. However, the calculated magnetic moments are much smaller of about 3.83 μ_B, 2.40 μ_B and 1.55 μ_B for Fe, Co and Ni atom, respectively. It is obviously arised from the hybridization of S-3*p* and Cu-3*d* states with *M* ions resulting that the magnetic moment spreads over the neighboring S and Cu atoms, as shown in table 2. The Co ions induce negative moments on the S atoms and Cu atoms with 0.20 μ_B and 0.35 μ_B, respectively. While, the S atoms and Cu atoms have a positive moment for Fe and Ni doped $CuGaS_2$. The magnetic moment on Ga atoms is very small in all the doped materials.

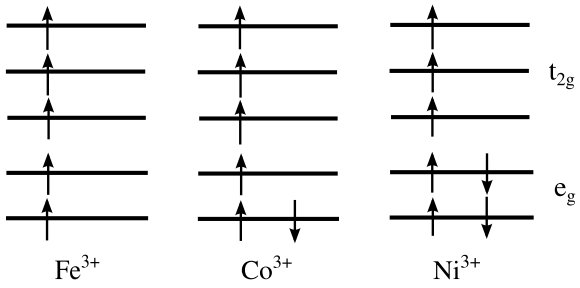

Fig. 5 Schematically show of the orbital occupation of 3*d* electron for *M* dopant in $CuGaS_2$.

Table 2 The average magnetic moment μ_B/atom for *M*, Ga, Cu and S atom in $Cu_4Ga_3MS_8$ systems (in μ_B).

$Cu_4Ga_3MS_8$	Ga	Cu	S	*M*
Fe	0.039	0.222	0.498	3.833
Co	0.015	-0.346	-0.204	2.401
Ni	0.013	0.361	0.727	1.550

3.2 Optical properties

We compare the optical absorption coefficients and optical conductivities of host $CuGaS_2$ semiconductor with the *M*-doped systems in polarizations, which has a close connection with the dielectric function. The computational formulas we use are as follows:

$$\varepsilon_1(\omega) = n^2(\omega) - \kappa^2(\omega) \quad (1)$$

$$\varepsilon_2(\omega) = 2n(\omega)\kappa(\omega) \quad (2)$$

$$\alpha(\omega) = \frac{2\omega \cdot \kappa(\omega)}{c} = \frac{\omega}{c}\sqrt{2(\sqrt{\varepsilon_1^2(\omega)+\varepsilon_2^2(\omega)} - \varepsilon_1(\omega))} \quad (3)$$

where the $\varepsilon_1(\omega)$ and $\varepsilon_2(\omega)$ are the real part and imaginary part, respectively. They are connected through the Kramers-Kronig relationship. From $\varepsilon_1(\omega)$ and $\varepsilon_2(\omega)$, the other optical properties, such as the refractive index $n(\omega)$, the extinction coefficient $\kappa(\omega)$ and the absorption coefficient $\alpha(\omega)$ can be evaluated.

The $\alpha(\omega)$ as a function of incident energy is shown in Fig. 6(a)-(c) for the energy range relevant to absorption of solar

RSC Advances Accepted Manuscript

This journal is © The Royal Society of Chemistry [year]

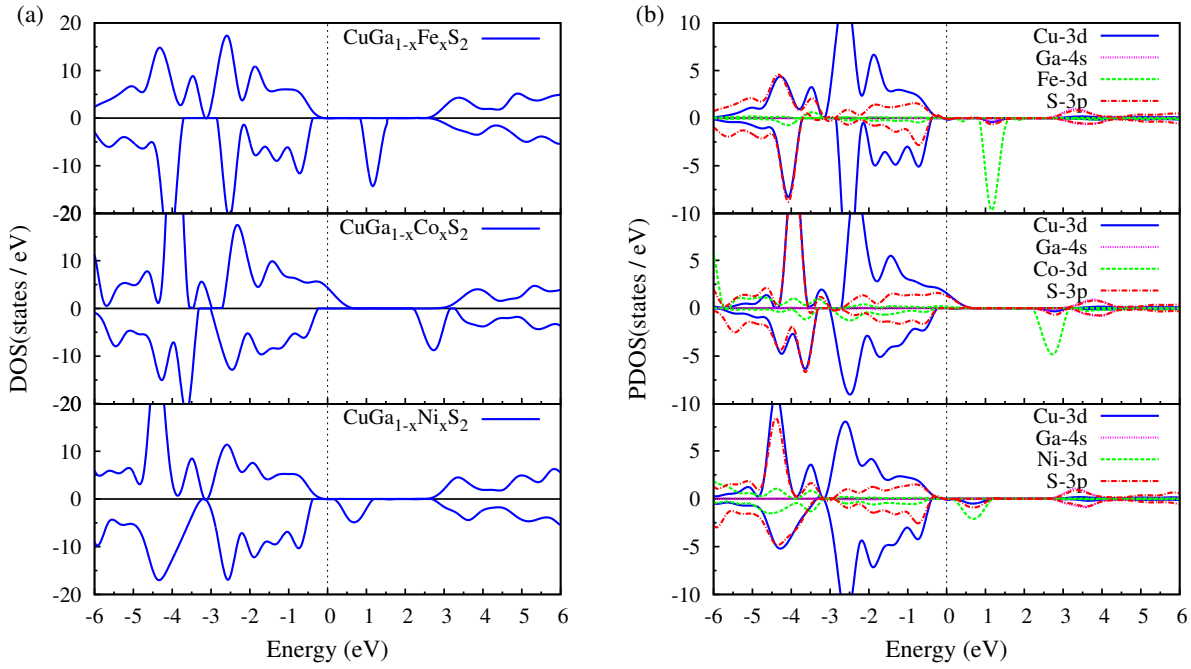

Fig. 4 (a) DOS and (b) PDOS of *M* (Fe, Co, Ni) doped $CuGaS_2$. The vertical dashed line is the Fermi level.

light. Since $CuGaS_2$ belongs to the tetragonal system, we consider the optical absorption only in two directions. Obviously, the optical absorption in the zz direction (along the c axis) is stronger than that in the xx direction (along the a axis). Therefore the subsequent discussion will be focused on the zz direction. The spectrum of the host chalcopyrite $CuGaS_2$ has the usual absorption peak at the theoretical value of the bandgap about 2.0 eV. However, for the Fe-doped $CuGaS_2$ compound, except the peak at 2.0 eV, two additional new absorption peaks appear at around 1.0 eV and 1.7 eV, corresponding to electron transition from VB to IB for both spin components. Besides, the optical absorption begins at almost zero energy, largely extending to the infrared portion of the solar spectrum, and the overall optical absorption intensity is greatly enhanced compared to that of host $CuGaS_2$. The result is in good agreement with the experimental result that two absorption peaks are observed at 1.2 eV and 1.9 eV.[20,27] Co-doped $CuGaS_2$ turns into a half-metal with the disappearance of absorption peak at 2.0 eV. The absorption enhancement at lower energy is caused by the electron transition from occupied states to unoccupied states around the Fermi level. As for Ni-substituted $CuGaS_2$, one absorption peak locates at about 1.75 eV, resulted from the same spin electron transition from VB to IB (see Fig. 6). The absorption spectrum of Ni-doped $CuGaS_2$ is also largely enhanced in intensity though with a relatively narrow energy range. Further more, the optical conductivity as shown in Fig. 6(d)-(f) has the same trend with the absorption coefficient according to $\sigma \propto \omega\varepsilon_2(\omega)$.

Strictly speaking, the IB needs to be partially filled so that a three-photon absorption process can happen. Though the IB obtained by doping Fe or Ni is empty, which can only enable VB-CB and VB-IB optical transition, a design with a third electrode for extracting current from the IB can relax the stringent requirement.[38] Besides, electrons excited from the VB to IB can transfer to CB through a nonequilibrium transition by absorbing a second photon. In a word, the Fe or Ni doped $CuGaS_2$ compound exhibits very excellent characteristics with the extended absorption energy range and the enhanced optical absorption intensity, due to the existence of isolated IBs. Thus the Fe or Ni doped $CuGaS_2$ may realize IBSCs with high quantum efficiencies.

4 Conclusions

In this work, we investigate the electronic structures and optical properties of host $CuGaS_2$ and 25% *M* (Fe, Co, Ni) doped $CuGaS_2$ by employing the range-separated hybrid functional Heyd-Scuseria-Ernzerhof (HSE06). Our results reveal that HSE06 can give a much better description of the host $CuGaS_2$ than DFT. Isolated intermediate bands (IBs) with optimal position and width appear in Fe or Ni doped $CuGaS_2$ compound,

RSC Advances Accepted Manuscript

which originate from the M-3d states with a weak hybridization of S-3p and Cu-3d states. Benefited from the two photons process induced by IBs, additional peaks appear in the spectrum. Besides, the optical absorption coefficients are greatly enhanced and the absorption energy ranges are largely extended in the M-doped $CuGaS_2$ systems. However, Co doping turns the system into a half-metal. Therefore, Fe or Ni doped $CuGaS_2$ semiconductor, will be a potential candidates for photovoltaic materials. Additionally, these materials may also be useful in other applications, such as photon up/down converters, spintronics and so on.

Acknowledgements

This work has been supported by the special Funds for Major State Basic Research Project of China (973) under Grant No. 2012CB933702, the NSF of China under Grant Nos. 11204310 and U1230202 (NSAF) and Heifei Center for Physical Science and Technology under Grant No. 2012FXZY004. The calculations are performed in Center for Computational Science of CASHIPS, the ScGrid of Supercomputing Center and Computer Net work Information Center of Chinese Academy of Science.

References

1 A. Luque and A. Martí, *Phys. Rev. Lett*, 1997, **78**, 5014–5017.
2 W. Shockley and H. J. Queisser, *J. Appl. Phys.*, 1961, **32**, 510–519.
3 T. Nozawa and Y. Arakawa, *Appl. Phys. Let.*, 2011, **98**, 171108.
4 I. Aguilera, P. Palacios and P. Wahnón, *Thin Solid Films*, 2008, **516**, 7055–7059.
5 I. Aguilera, Palacios and P. Wahnón, *Sol. Energy Mater. Sol. Cells*, 2010, **94**, 1903–1906.
6 P. Chen, M. Qin, H. Chen, C. Yang, Y. Wang and F. Huang, *Phys. Status Solidi A*, 2013, **210**, 1098–1102.
7 A. Luque and A. Martí, *Adv. Mater*, 2010, **22**, 160.
8 P. Wahnón and C. Tablero, *Phys. Rev. B*, 2002, **65**, 165115.
9 C. Tablero, *Phys. Rev. B*, 2005, **72**, 035213.
10 C. Tablero, *Sol. Energy Mater. Sol. Cells*, 2006, **90**, 588.
11 P. Palacios, I. Aguilera, K. Sánchez, J. C. Conesa and P. Wahnón, *Phys. Rev. Lett.*, 2008, **101**, 046403.
12 Martí, Antonio, M. D. Fuertes and A. Luque, *J. Appl. Phys.*, 2008, **103**, 073706.
13 I. Aguilera, J. Vidal, P. Wahnón, L. Reining and S. Botti, *Phys. Rev. B*, 2011, **84**, 085145.
14 P. Palacios, K. Sánche, J. C. Conesa and P. Wahnón, *Phys. Status Solidi A*, 2006, **203**, 1395–1401.
15 P. Palacios, K. Sánche, J. C. Conesa, J. J. Fernández and P. Wahnón, *Thin Solid Films*, 2007, **515**, 6280–6284.
16 C. Tablero, *J. Appl. Phys.*, 2009, **106**, 073718.
17 C. Tablero, *Thin Solid Films*, 2010, **519**, 1435.
18 X. Lv, S. Yang, M. Li, H. Li, J. Yi, M. Wang and J. Zhong, *Solar Energy*, 2014, **103**, 480–487.
19 C. Yang, M. Qin, Y. Wang, D. Wan, F. Huang and J. Lin, *Sci. Rep.*, 2013, **3**, 1286.
20 Marsen, Björn, Klemz, Sascha, U. Thomas, Schock and Hans-Werner, *Pro. Photovoltaics: Research and Applications*, 2012, **20**, 625–629.
21 D. F. Marrón, A. Martí and A. Luque, *Phys. Status Solidi A*, 2009, **206**, 1021–1025.
22 Y.-J. Zhao and A. Zunger, *Phys. Rev. B*, 2004, **69**, 075208.
23 P. Palacios, I. Aguilera, P. Wahnón and J. C.Conesa, *J. Phys. Chem. C*, 2008, **112**, 9225.
24 Donghan and Y.Y.Sun, *Phys. Rev. B*, 2013, **87**, 155206.
25 J. Pohl and K. Albe, *Phys. Rev. B*, 2013, **87**, 245203.
26 *Ternary Chalcopyrite Semiconductors: Growth Electronic Properties and Applications*, ed. J. L. Shay, J. H. Wernick and B. R. Pamplin, Pergamon Press, Oxford, New York, 1st edn, 1975, pp. 110–128.
27 T. Teranishi, K. Sato and K. Knodo, *Journal of the Physical Society of Japan*, 1974, **36**, 1618–1624.
28 A. Luque, A. Martí, E. Antolín and C. Tablero, *Physica B*, 2006, **382**, 320–327.
29 G. Kresse and J. Furthmüller, *Comput. Mater. Sci*, 1996, **6**, 15–50.
30 J. P. Perdew, K. Burkeand and M. Ernzerhof, *Phys. Rev.Lett*, 1996, **77**, 3865.
31 P. E. Blöchl, *Phys. Rev. B*, 1994, **50**, 17953.
32 J. Heyd, G. E. Scuseria and M. Ernzerho, *J. Chem. Phys.*, 2003, **118**, 8207.
33 J. Heyd, G. E. Scuseria and M. Ernzerho, *J. Chem. Phys.*, 2006, **124**, 219906.
34 H. J. Monkhorst and J. D. Pack, *Phys. Rev. B*, 1976, **13**, 5188.
35 S. Laksari, A. Chahed, N. Abbouni, O. Benhelal and B. Abbar, *Comp. Mat. Sci.*, 2006, **38**, 223.
36 J. E. Jaffe and A.Zunger, *Phys. Rev. B*, 1983, **28**, 5822.
37 C. Tablero and D. F. Marrón, *J. Phys. Chem. C*, 2010, **114**, 2756–2763.
38 F. Wu and H. Lan, *J. Chem. Phys.*, 2012, **137**, 104702.

RSC Advances Accepted Manuscript

This journal is © The Royal Society of Chemistry [year]

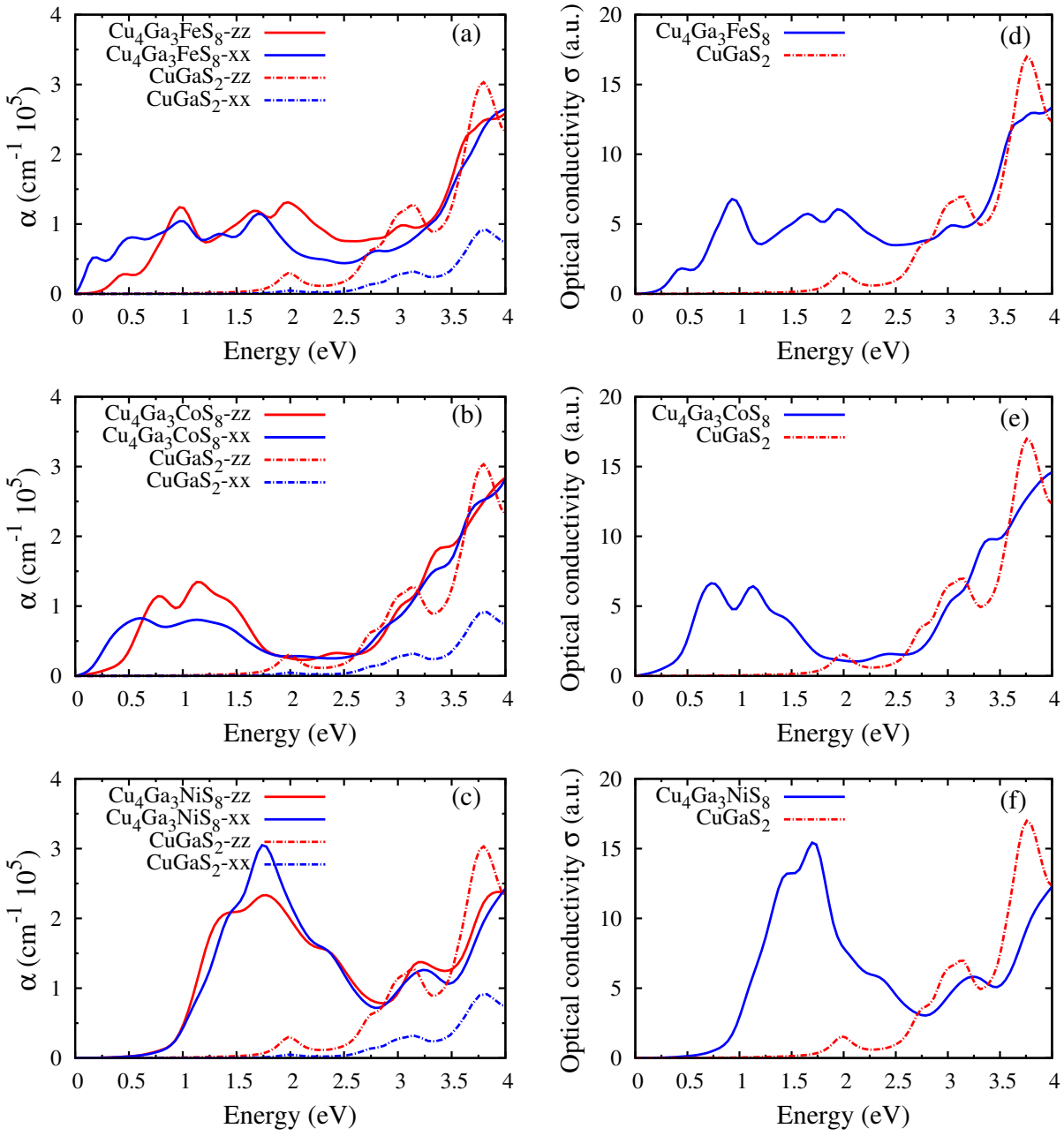

Fig. 6 Comparision of optical absorption coefficient and optical conductivity between $Cu_4Ga_3MS_8$ and $CuGaS_2$.

RSC Advances Accepted Manuscript

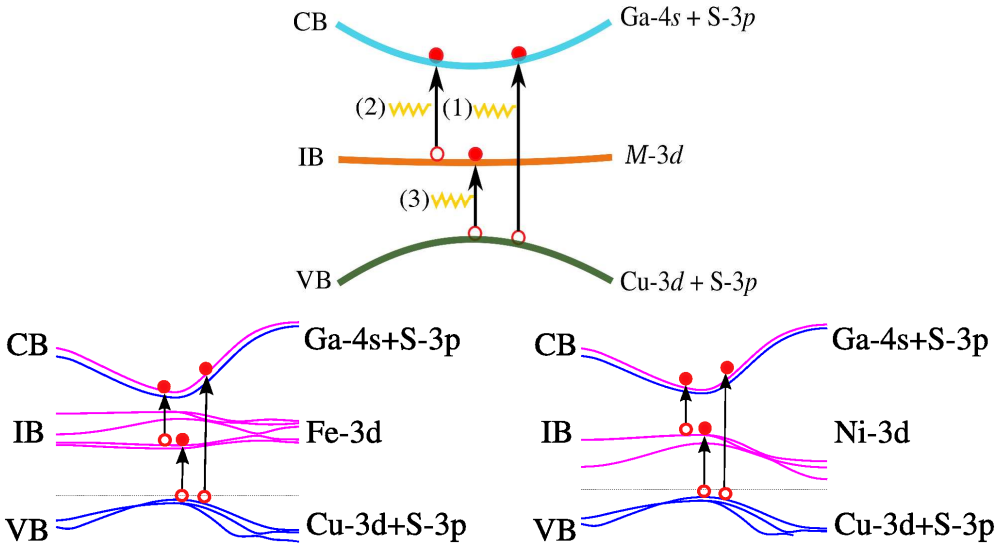

M (Fe、Co、Ni) doped $CuGaS_2$ are systematically investigated by using the screened-exchange hybrid density functional theory, which show that Fe and Ni doped $CuGaS_2$ are potential candidates for photovoltaic area.

RSC Advances Accepted Manuscript